

Electric field effect on superconductivity in atomically thin flakes of NbSe₂

Neal E. Staley, Jian Wu, Peter Eklund, and Ying Liu*

Department of Physics, The Pennsylvania State University, University Park, Pennsylvania 16802, USA

Linjun Li and Zhuan Xu

Department of Physics, Zhejiang University, Hangzhou 310027, People's Republic of China

(Received 14 December 2008; revised manuscript received 12 October 2009; published 12 November 2009)

We studied the electric field effect on superconductivity in atomically thin flakes of NbSe₂ prepared by mechanical exfoliation. We found that these NbSe₂ flakes are superconducting down to a thickness of a single unit cell consisting of two molecular layers of NbSe₂ with an onset superconducting transition temperature (T_c) up to 2.5 K. We demonstrated that the T_c of the thinnest flakes can be modulated by an applied gate voltage with a T_c shift as large as 200 mK, which is larger than expected from a simple consideration based on Bardeen-Cooper-Schrieffer theory. We discuss the possible reasons for the observed enhanced electric field modulation of T_c .

DOI: [10.1103/PhysRevB.80.184505](https://doi.org/10.1103/PhysRevB.80.184505)

PACS number(s): 74.62.Yb, 74.25.Fy, 74.78.Db

I. INTRODUCTION

Physical properties of a superconducting material such as its superconducting transition temperature (T_c) can be controlled by its charge-carrier density. Chemical doping is a popular method for modulating the charge-carrier density. However, doping may induce unwanted chemical, structural, or other changes to the material. Furthermore, it will introduce disorder. As a consequence, it is often difficult to quantify the effect on superconducting properties that is purely due to induced carrier density change from doping. For two-dimensional (2D) superconducting systems such as ultrathin films, on the other hand, the carrier density can be changed by an electric field effect, a technique that minimizes the potential complications of chemical doping. This technique was first used to modulate the T_c of quench condensed thin superconducting films of Bi.¹ More recently, it was used to study ultrathin films of high- T_c superconductors grown epitaxially using molecular-beam epitaxy (MBE) or pulsed laser deposition (PLD).²⁻⁴ Remarkably, full switching from insulating to superconducting behavior was demonstrated in amorphous Bi films⁵ as well as in an interface superconductor of transition-metal oxides,⁶ making it possible to envision the realization of superconducting field-effect transistors.

The study of the electric field effect of superconductivity requires the use of ultrathin superconducting films because the carrier density for most superconducting materials is high, so that only the charge carriers in a very thin layer of the superconductor can be modulated by an electric field. Even for an ultrathin film, the fraction of charge-carrier density change may still be rather minimal. Therefore controlling superconductivity by electric field effect in ultrathin films also requires the use of high-quality dielectrics. For such electric field effect devices, the interface between the film and the substrate and that between the film and the dielectric rather than the intrinsic properties of the superconducting material may dominate the behavior of the device. Here we demonstrate an alternate approach to the electric field effect of superconductivity by the use of atomically thin NbSe₂ flakes prepared by the mechanical exfoliation of a

superconducting single crystal of NbSe₂ and the deposition of the flakes onto an atomically flat, heavily doped Si substrate with a thermally grown layer of SiO₂. Different from previous approaches to the electric field effect on superconductivity, these flakes feature an approximate crystalline structure, which makes it possible for the material to possess an electronic band structure similar to the bulk. Furthermore, this technique may avoid potential problems originating from the interfaces prepared by conventional deposition techniques such as MBE or PLD, including mechanical strains and interface electronic reconstruction.

NbSe₂ has a layered crystalline structure with the unit cell of 2H NbSe₂ consisting of two NbSe₂ layers in *ABAB...* stacking. The crystal bonding between the NbSe₂ layers are van der Waals in nature. Each NbSe₂ layer in turn contains one Nb and two Se layers in the sequence of Se-Nb-Se, featuring a covalent bond between the Nb and Se. When cleaved, the ending layer is usually a Se sheet.⁷ The electronic band-structure calculation and measurements on 2H NbSe₂ revealed multiple bands crossing the Fermi surface.⁸⁻¹¹ One of these bands features charge-density waves with an onset temperature 32 K (Ref. 12) and the other two show superconductivity with a T_c of 7.2 K. Interestingly, different superconducting energy gaps on these two bands¹⁰ were found with the large and the small energy gaps 1.22 and 1.13 meV, respectively. However, a more recent study appears to suggest that superconductivity and charge-density waves may coexist in the same bands.¹³ It is evident that this material provides a rich system for studying the effect of a band structure on superconducting properties and the interplay between superconductivity and charge-density waves in the 2D limit, the latter of which has never been addressed previously.

An early study of thin flakes of NbSe₂ revealed a decreasing T_c as the thickness of the flake is reduced. However, the value of the flake thickness was not measured directly.⁷ In a more recent study, ultrathin flakes of NbSe₂ down to a single molecular layer were fabricated, with a rather low mobility, (~ 1 cm²/V s at room temperature and complete absence of superconductivity).¹⁴ The carrier density in this early study of single molecular layer NbSe₂ was found to be very differ-

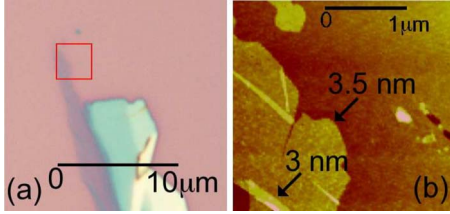


FIG. 1. (Color online) (a) Optical image of one-unit-cell-thick NbSe₂ crystal connected to a thick flake. Note that different color bands correspond to different thicknesses. (b) AFM image of the boxed region in (a) showing a step height of 3.5 nm between flake and substrate and double fold with a step height of 3.0 nm. The AFM imaging suggests that the flake is one-unit-cell thick, containing two molecular sheets of NbSe₂.

ent from that in bulk 2H NbSe₂, roughly $1.6 \times 10^{22} \text{ cm}^{-3}$.¹⁵ Given that the spacing between adjacent NbSe₂ layers is 6.3 Å, the 2D charge-carrier density per NbSe₂ sheet n is on the order of $1 \times 10^{15} \text{ cm}^{-2}$, well above what is obtainable using conventional dielectrics such as the 300-nm-thick SiO₂ dielectric used in this study, with a maximum charge-carrier density modulation around $\Delta n \sim 10^{13} \text{ cm}^{-2}$. As a result we expect a small carrier-density change, $\Delta n/n \sim 10^{-2}$, and a correspondingly small T_c modulation.

II. EXPERIMENT

Single-crystal NbSe₂ was grown by iodine vapor transport and characterized structurally by x-ray diffraction. The bulk samples had a residual resistivity ratio (RRR) of 10 and a superconducting T_c of 7.2 K. No signature for the charge-density wave (CDW) transition at 32 K was observed in the electrical transport measurement, as expected for NbSe₂ crystals with a RRR of 10. Crystals with a much higher RRR, probably around 30 or higher, are needed to observe a CDW anomaly in the temperature-dependent resistivity.¹⁶ Using a simple micromechanical exfoliation technique as described by Ref. 14, we created atomically thin flakes of this material with micron-sized lateral dimensions. This technique involves first cleaving the bulk single-crystal NbSe₂ using an adhesive (Scotch tape) and pressing the peeled-off crystal against a Si/SiO₂ substrate (300 nm thermally grown SiO₂ on highly n -doped Si). Thin flakes can be identified under an optical microscope [Fig. 1(a)]. As the thickness of the flake is reduced, discretized color/faintness is observed, allowing a “color code” to be developed. Atomic force microscope (AFM) measurements of these flakes [Fig. 1(b)] can, in principle, correlate the color and the faintness of the flakes with the flake thickness. Similar to what was observed in graphene studies, NbSe₂ flakes appear to also “float” on the substrate with a finite distance between the substrate and the flakes. This offset is sample dependent and difficult to quantify. As a result, the flake thickness cannot be determined accurately by measuring between the flake and substrate alone. Occasionally, folds of the flake may be found [Fig. 1(b)], in which case the flake thickness based upon the height of the folds above the flat surface of the flake appears to be rather accurate, which was used to calibrate our color code of the flake thickness.

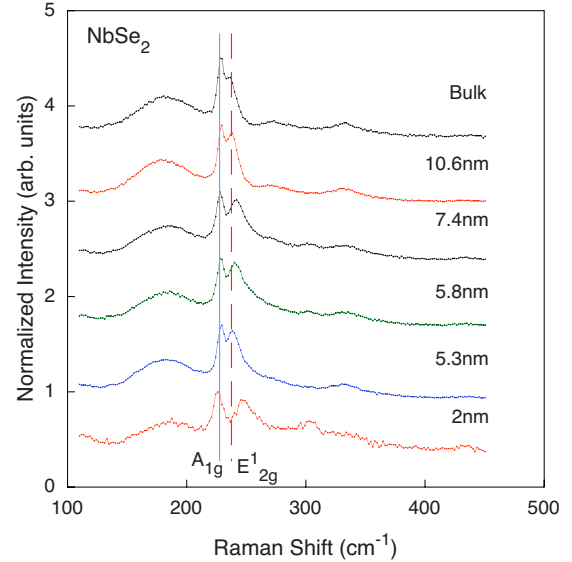


FIG. 2. (Color online) Raman spectra of flakes of differing thicknesses as measured by AFM. The intensity is normalized for clarity. Note that the laser power used for the 2-nm-thick flake was five times lower than that for the bulk crystals. The blue (solid) line indicates the position of the A_{1g} mode and the red (dashed) that of the E_{2g}^1 mode in the bulk. The apparent peak at 178 cm^{-1} may be attributed to a two-phonon process.

To further characterize the NbSe₂ flakes we performed Raman spectroscopy measurements as a function of flake thickness. This study on micron-sized ultrathin flakes shown in Fig. 2, employed a laser power of 0.06 mW, wavelength of 514.5 nm and a spot size of 600 nm. Our data shows that the two phonon peaks, A_{1g} centered at 228 cm^{-1} (Ref. 17) (corresponding to an out-of-plane mode) and the E_{2g}^1 centered at 237 cm^{-1} (Ref. 17) (corresponding to an in-plane mode) shift as the thickness of the NbSe₂ flake is reduced. The E_{2g}^1 peak experiences the largest shift of 10 cm^{-1} which begins to deviate from bulk values even for the thick flakes we studied. The A_{1g} mode was found to shift to 224 cm^{-1} (compared with the bulk value of 228 cm^{-1}) but in a nonsystematic way and only in the thinnest flakes. The physical origin of the observed Raman shift is not understood. Raman peak shifts have previously been used to identify graphene flake thickness.^{18,19} But the application of the same method to NbSe₂ flakes is problematic as evidenced by the nonmonotonic changes in Raman shift as the thickness was reduced. Furthermore, even the modest laser excitation of 0.06 mW was found to result in physical damage to a ultrathin NbSe₂ flake. Consequently Raman spectroscopy becomes no longer a nondestructive method of characterizing NbSe₂ flakes.

Electric field effect devices of NbSe₂ flakes were fabricated using an all-dry, lithography free technique. A thin quartz filament with a diameter of $\sim 1 \mu\text{m}$ was placed on top of the flake and used as a shadow mask.²⁰ Flakes used for this study were on average 2–3 μm in lateral dimensions, smaller than the typical size of graphene flakes. Two-terminal devices with the source and the drain having a contact areas on the order of $1 \mu\text{m}^2$ were fabricated for this study. Devices were measured by a dc technique with an applied current density $\sim 1 \times 10^5 \text{ A/cm}^2$. The contact resis-

TABLE I. Summary of parameters of samples used in the present study.

Thickness	RRR	Onset T_c (K)
Bulk	10.5	7.2
10 nm	6.7	5.7
5.5 nm	2.7	5.0
2–3 sheet ^a	1.7	<4.2

^aFrom color code.

tance between leads and flake could not be quantified because of the two-terminal device geometry. The n -doped silicon below a 300-nm-thick SiO_2 top layer was used as a back gate, producing $7 \times 10^{10} \text{ cm}^{-2}/\text{V}$. All devices measured in this study had the NbSe_2 connected to the positive polarity for the application of a gate voltage, meaning that applying a positive gate voltage corresponds to adding holes to the flake.

III. RESULTS

In order to characterize our NbSe_2 flakes we measured their electrical transport properties from room temperature down to 4.2 K as a function of the flake thickness. Measurements on bulk NbSe_2 were performed in the usual four-point geometry, while flake measurements were done using the lithography free technique, which gives a quasi four-point geometry including the contact resistance between the flake and the gold film as described above. The lithography free technique cannot be used for very thick flakes, because the filament cannot be brought sufficiently close to the flake, causing incomplete shadowing, therefore the thickest flake studied was 10 nm thick. As we reduce the thickness from bulk to ~ 2 –3 sheets (based on our color code), the RRR and superconducting T_c are reduced systematically (Table I). Note that even the very thick 10 nm flake has a reduced onset T_c of 5.7 K compared to the bulk value of 7.2 K. The resistance for flake samples is not expected to reach zero due to the roughly constant contact resistance in series with the sample. As the thickness is decreased, the resistive transition becomes further depressed and broadened, with the 5.5 nm flakes having an onset T_c of 5 K, and a broad transition such that at 4.2 K the resistive transition is not complete [Fig. 3, inset (a)]. The (2–3)-molecular sheet thick, as-prepared flakes (the thinnest that we studied) were found to show insulating behavior down to 20 mK [Fig. 3 inset (b)]. Similar results were found in three different devices, consistent with what was previously reported.¹⁴

This suppression of the T_c in superconducting thin films as the film thickness is reduced is well known, having been studied in ultrathin films sequentially deposited at liquid helium temperature (quench deposition),^{21–23} and disordered films deposited at room temperature.^{24–27} As the thickness is reduced, disorder and interaction effects reduce the charge-carrier density, leading to reduced electron screening and enhanced Coulomb interaction causing the superconducting T_c

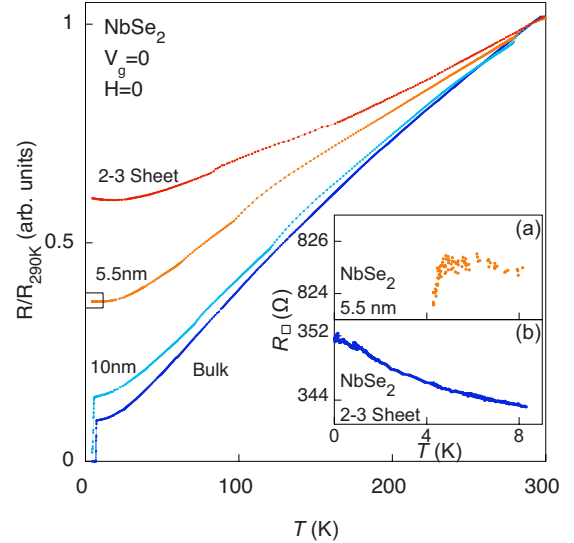


FIG. 3. (Color online) Normalized resistance (R) vs temperature (T) showing that the RRR and onset T_c decrease monotonically simultaneously as the flake thickness is reduced. Relevant parameters are summarized in Table I. Insets: (a) details of 5.5 nm boxed region; (b) R vs T for an as-prepared (2–3)-molecular sheet NbSe_2 flake with insulating behavior down to $T=20$ mK.

to be suppressed. At sufficiently high disorder superconductivity is completely suppressed leading to an insulating state. In the intermediate regime, as the disorder is increased the temperatures required for true zero resistance may become experimentally unachievable. Furthermore, the lowest electronic temperatures can be limited by the inability to properly cool the electrons in the system.²⁸ However, the systematic reduction in superconducting T_c that we observed as the thickness was decreased, shown in Fig. 3, allows us to conclude that even though the resistance drop we observed is rather modest down to our base temperature, the resistance drop still originates from superconductivity.

We estimated the mobility of our devices in order to see how disordered our devices were. Since our samples were two-terminal devices, we were unable to measure the Hall mobility. However, the field effect mobility (μ_{FE}) can be obtained from the induced charge via the back gate.²⁹ We found that our devices had μ_{FE} in the range of 10 – $60 \text{ cm}^2/\text{V s}$, which are higher than the 0.4 – $6 \text{ cm}^2/\text{V s}$ reported previously.¹⁴ On the other hand, the normal-state sheet resistance were found to vary from flake to flake in a nonsystematic way, perhaps due to unintentional doping or defect formation from exfoliation, or to the uncontrolled contact resistance.

We attempted to improve the mobility of our devices by reducing the amount of disorder. In graphene flakes, it was found that unintentional doping in air, most likely water adsorbates, degrades the mobility of graphene flakes.³⁰ We employed a similar high-current cleaning technique used in graphene research.³¹ In this process, we first heated the samples to greater than the T_c of NbSe_2 (7.2 K) to ensure that the flake was in the normal state. A current steadily increasing from a fixed low to a fixed high value was then applied to the device. After each current sweep, the device was mea-

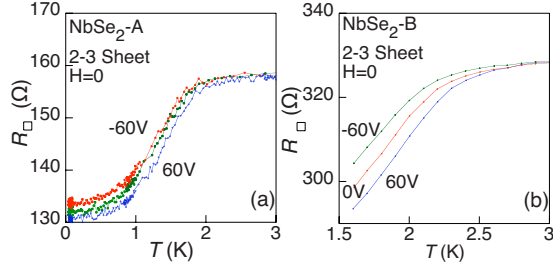


FIG. 4. (Color online) (a) Resistance (R) vs temperature (T) of a 2–3 sheet NbSe₂ sample after cleaning showing an onset of superconductivity at 2 K and an electric field induced shift in T_c of \sim up to 120 mK. Note that the level off below 1 K is dependent on sourcing current, attributable to heating of the flake, possibly because the flake is free standing above the substrate; (b) R vs T of another 2–3 sheet NbSe₂ flake after cleaning showing an onset T_c of 2.5 K and a T_c shift of up to 200 mK. In both cases the total carrier density change was $8 \times 10^{12}/\text{cm}^2$.

sured and mobility calculated. The maximum current used for cleaning purposes was 2 mA across a 1- μm -wide (1.5- μm -long) 2–3 sheet flake, corresponding to a current density of at least 1×10^8 A/cm². We believe that the high current likely cleaned the device by Joule heating. The flake was at a significantly high temperature, evaporating absorbates that were then cryopumped away. It is also possible that the high current caused electromigration that helped remove particulate and structural defects.

After cleaning the devices a superconducting transition was observed in our thinnest samples (\sim 2–3 molecular sheets) as shown in Fig. 4. Slightly different values for the onset T_c , 2 and 2.5 K, respectively, were observed for two samples. The reduction in onset T_c and transition broadening is consistent with what was observed for thicker flakes shown in Fig. 3. Magnetoresistance measurements (Fig. 5) indicate a $\mu_0 H_{c\perp}$ of \sim 1 T.³² The application of gate voltage was found to lead to a substantial change in T_c . In order to quantify the change in T_c due to electric field modulation, we choose the temperature at which the resistance is 90% of the normal-state resistance to quantify the change in T_c . Using this definition, an observed T_c modulation of 120 mK for sample A and 200 mK for sample B was found, corresponding to a $\frac{\Delta T_c}{T_{c0}}$ of 6% and 8%, respectively, under a total charge-carrier density change of $8.4 \times 10^{12}/\text{cm}^2$.

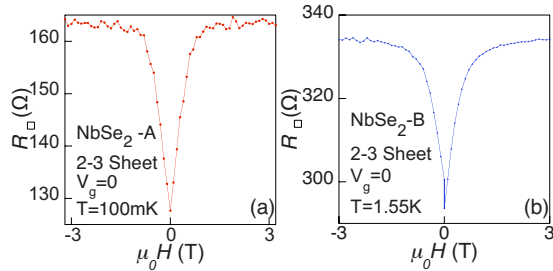


FIG. 5. (Color online) (a) Resistance vs magnetic field applied perpendicular to the sheets of a 2–3 sheet NbSe₂ sample at 100 mK after cleaning showing a $\mu_0 H_{c\perp}$ of 1 T; (b) R vs H_{\perp} at 1.55 K of another 2–3 sheet NbSe₂ flake after cleaning showing a $\mu_0 H_{c\perp}$ of 1.2 T.

IV. DISCUSSION AND CONCLUSION

Bulk NbSe₂ is a weak-coupled superconductor.³³ Therefore we apply a simple weak-coupling Bardeen-Cooper-Schrieffer (BCS) theory to estimate the modulation of T_c by the carrier-density modulation. For simplicity we start with a single-band model with its T_c modulation given by

$$\left| \frac{\delta T_c}{T_{c0}} \right| = \frac{1}{N(0)V} \frac{\delta N(0)}{N(0)} \quad (1)$$

and

$$N(0)V = -1/\ln\left(\frac{T_{c0}}{1.14\Theta_D}\right), \quad (2)$$

where δT_c is the change in T_c with charging, T_{c0} is the initial T_c , $N(0)$ is the initial superconducting charge-carrier density, Θ_D is the Debye temperature, and V is the electron-phonon coupling strength, we further assume that in the single-band model the change in superconducting fraction $\frac{\delta N(0)}{N(0)}$ is equal to the fractional change in total charge

$$\frac{\delta N(0)}{N(0)} \approx \left(\frac{\delta n}{n} \right)_{total}. \quad (3)$$

Using a bulk T_c of 7.2 K, Θ_D of 224 K,³⁴ and a carrier density $n=8.51 \times 10^{14}/\text{cm}^2$ per sheet,³⁵ we estimate that a $\frac{\Delta T_c}{T_{c0}}$ change of 3.6% for a flake of a unit cell of NbSe₂ (two NbSe₂ sheets) is expected, smaller than the (6–8 %) change observed in our experiment.

However this estimate based on the BCS theory may be overly simplified. It is possible that the crystallinity, and therefore the presence of a band structure, of our flakes needs to be taken into account. Given that NbSe₂ has both electron and hole bands crossing the Fermi energy,^{8,9} the charge-carrier densities of these bands are different from one another. We know that the Fermi energy must remain the same across all bands during charging. Since the density of states is different from band to band in general, it is possible for the charge-carrier density change of each band to be different from the total charge-carrier density change. Specifically, as a gate electric field is applied, the carrier density change of each band may be different from the total carrier density change to ensure that the Fermi energy remains the same for all bands during charging because the density of states at the Fermi energy is likely to differ from band to band. However, details on the density of states for all bands crossing the Fermi surface are not available in the literature, making it difficult to estimate the T_c modulation of each individual band quantitatively.

An enhanced $\frac{\Delta T_c}{T_{c0}}$ could also be due to a lower effective charge-carrier density, this could be achieved by freezing out the carriers as charge-density waves set in. The interplay between superconductivity and charge-density waves in NbSe₂ has not been fully understood, even in the bulk. Angle-resolved photoemission spectroscopy measurements have indicated that only two of the NbSe₂ bands are superconducting¹⁰ and the CDW may occur on the nonsuperconducting band.¹² More recent measurements seem to suggest that CDW may exist on the superconducting bands and

competes with superconductivity.¹³ The presence of CDW reduces charge carriers available for superconductivity in this material, which could explain the large T_c modulation observed in our experiments.

As shown above a T_c suppression was found in atomically thin flakes of NbSe₂. This reduction in T_c could be due to an enhanced Coulomb interaction. Because of this, the NbSe₂ may become a strongly coupling superconductor in thin flakes. This material is predicted to be close to the strong-coupling superconductor even in the bulk.³⁶ For strong-coupling superconductor,³⁷ we expect that

$$T_c = \frac{\Theta_D}{1.45} \exp^{-1.04(1+\lambda)/\lambda - \mu^*(1+0.62\lambda)}, \quad (4)$$

where λ is the electron-phonon coupling constant corresponding to the $N(0)V$ in the BCS model and μ^* is the Coulomb coupling constant of Morel and Anderson³⁸

$$\mu^* = \frac{N(0)V_c}{1 + N(0)V_c \ln(E_B/\omega_0)}. \quad (5)$$

Since both λ and μ^* depend on the charge-carrier density, calculating the expected $\frac{\Delta T_c}{T_{c0}}$ is nontrivial. However, whether a crossover to strong-coupling superconductivity may help explain the observed high- $\frac{\Delta T_c}{T_{c0}}$ modulation needs to be resolved.

In conclusion, we developed a method for fabricating atomically thin flakes of superconducting NbSe₂. The thinnest as prepared flakes (2–3 NbSe₂ sheets) were not superconducting. These flakes were cleaned using high-current application at low temperatures, after which these flakes were found to exhibit superconductivity with an onset T_c as high as 2.5 K. Electric field effect studies on these 2–3 sheet devices demonstrated a change in superconducting transition temperature of ~ 200 mK for a charge-carrier density change of $8.4 \times 10^{12}/\text{cm}^2$, which corresponds to a $\frac{\Delta T_c}{T_{c0}}$ change of 6–8 %. This large observed field effect $\frac{\Delta T_c}{T_{c0}}$ change cannot be explained by a simple BCS theory. We suggest that the observed large electric field effect could be due to either a band-dependent electric field effect of superconductivity or a transition from a weak-coupling to a strong-coupling superconductor as the single crystal is thinned to atomic length scale. More work is needed to fully understand the effects of crystallinity on superconductivity in atomically thin flakes of NbSe₂ and to see if a single sheet of NbSe₂ is superconducting.

ACKNOWLEDGMENTS

We would like to acknowledge useful discussions with C. P. Puls, J. Zhu, and A. M. Goldman. This work is supported at Penn State by DOE under Grant No. DE-FG02-04ER46159, DOD ARO under Grant No. W911NF-07-1-0182, and at Zhejiang University by NSFC under Grant No. 10628408.

*liu@phys.psu.edu

- ¹R. E. Glover and M. Sherrill, Phys. Rev. Lett. **5**, 248 (1960).
- ²C. H. Ahn, J. M. Triscone, and J. Mannhart, Nature (London) **424**, 1015 (2003).
- ³K. S. Takahashi, M. Gabay, D. Jaccard, K. Shibuya, T. Ohnishi, M. Lippmaa, and J. M. Triscone, Nature (London) **441**, 195 (2006).
- ⁴A. Cassinese, G. M. D. Luca, A. Prigiobbo, M. Salluzzo, and R. Vaglio, Appl. Phys. Lett. **84**, 3933 (2004).
- ⁵K. A. Parendo, K. H. Sarwa B. Tan, A. Bhattacharya, M. Eblen-Zayas, N. E. Staley, and A. M. Goldman, Phys. Rev. Lett. **94**, 197004 (2005).
- ⁶A. D. Caviglia, S. Gariglio, N. Reyren, D. Jaccard, T. Schneider, M. Gabay, S. Thiel, G. Hammerl, J. Mannhart, and J. M. Triscone, Nature (London) **456**, 624 (2008).
- ⁷R. F. Frindt, Phys. Rev. Lett. **28**, 299 (1972).
- ⁸R. Corcoran, P. Meeson, Y. Onuki, P. A. Probst, M. Springford, K. Takata, H. Harima, G. Y. Guo, and B. L. Gyorffy, J. Phys.: Condens. Matter **6**, 4479 (1994).
- ⁹L. F. Mattheiss, Phys. Rev. B **8**, 3719 (1973).
- ¹⁰T. Yokoya, T. Kiss, A. Chainani, S. Shin, M. Nohara, and H. Takagi, Science **294**, 2518 (2001).
- ¹¹D. W. Shen, Y. Zhang, L. X. Yang, J. Wei, H. W. Ou, J. K. Dong, B. P. Xie, C. He, J. F. Zhao, B. Zhou, M. Arita, K. Shimada, H. Namatame, M. Taniguchi, J. Shi, and D. L. Feng, Phys. Rev. Lett. **101**, 226406 (2008).
- ¹²D. S. Inosov, V. B. Zabolotnyy, D. V. Evtushinsky, A. A.

- Kordyuk, B. Büchner, R. Follath, H. Berger, and S. V. Borisenko, New J. Phys. **10**, 125027 (2008).
- ¹³S. V. Borisenko, A. A. Kordyuk, Z. B. Zabolotnyy, D. S. Inosov, D. Evtushinsky, B. Buchner, A. N. Yaresko, A. Varykhalov, R. Follath, W. Eberhardt, L. Patthey, and H. Berger, Phys. Rev. Lett. **102**, 166402 (2009).
- ¹⁴K. S. Novoselov, D. Jiang, F. Schedin, T. J. Booth, V. V. Khotkevich, S. V. Morozov, and A. K. Geim, Proc. Natl. Acad. Sci. U.S.A. **102**, 10451 (2005).
- ¹⁵H. N. S. Lee, H. McKinzie, D. S. Tannhauser, and A. Wold, J. Appl. Phys. **40**, 602 (1969).
- ¹⁶K. Iwaya, T. Hanaguri, A. Koizumi, K. Takaki, A. Maeda, and K. Kitazawa, Physica B **329-333**, 1598 (2003).
- ¹⁷C. M. Pereira and W. Y. Liang, J. Phys. C **15**, L991 (1982).
- ¹⁸C. Stampfer, F. Molitor, D. Graf, K. Ensslin, A. Jungen, C. Hierold, and L. Wirtz, Appl. Phys. Lett. **91**, 241907 (2007).
- ¹⁹J. A. Robinson, C. P. Puls, N. E. Staley, J. P. Stitt, M. A. Fanton, K. V. Emtsev, T. Seyller, and Y. Liu, Nano Lett. **9**, 964 (2009).
- ²⁰N. Staley, H. Wang, C. Puls, J. Forster, T. Jackson, K. McCarthy, B. Clouser, and Y. Liu, Appl. Phys. Lett. **90**, 143518 (2007).
- ²¹D. B. Haviland, Y. Liu, and A. M. Goldman, Phys. Rev. Lett. **62**, 2180 (1989); A. M. Goldman and Y. Liu, Physica D **83**, 163 (1995).
- ²²M. Strongin, R. S. Thomson, O. F. Kammerer, and J. E. Crow, Phys. Rev. B **1**, 1078 (1970).
- ²³R. C. Dynes, J. P. Garno, and J. M. Rowell, Phys. Rev. Lett. **40**, 479 (1978).

- ²⁴A. F. Hebard and J. M. Vandenberg, *Phys. Rev. Lett.* **44**, 50 (1980).
- ²⁵A. Yazdani and A. Kapitulnik, *Phys. Rev. Lett.* **74**, 3037 (1995).
- ²⁶S. Okuma, T. Terashima, and N. Kukubo, *Phys. Rev. B* **58**, 2816 (1998).
- ²⁷A. F. Hebard and M. A. Paalanen, *Phys. Rev. B* **30**, 4063 (1984).
- ²⁸K. A. Parendo, K. H. Sarwa B. Tan, and A. M. Goldman, *Phys. Rev. B* **74**, 134517 (2006).
- ²⁹N. E. Staley, C. Puls, and Y. Liu, *Phys. Rev. B* **77**, 155429 (2008).
- ³⁰F. Schedin, A. K. Geim, S. V. Morozov, E. W. Hill, P. Blake, M. I. Katsnelson, and K. S. Novoselov, *Nature Mater.* **6**, 652 (2007).
- ³¹J. Moser, A. Berreiro, and A. Bachtold, *Appl. Phys. Lett.* **91**, 163513 (2007).
- ³²J. E. Graebner and M. Robbins, *Phys. Rev. Lett.* **36**, 422 (1976).
- ³³B. P. Clayman and R. F. Frindt, *Solid State Commun.* **9**, 1881 (1971).
- ³⁴C. L. Huang, J.-Y. Lin, Y. T. Chang, C. P. Sun, H. Y. Shen, C. C. Chou, H. Berger, T. K. Lee, and H. D. Yang, *Phys. Rev. B* **76**, 212504 (2007).
- ³⁵N. P. Ong, *Phys. Rev. B* **43**, 193 (1991).
- ³⁶K. Machida, *Prog. Theor. Phys.* **66**, 41 (1981).
- ³⁷W. L. McMillan, *Phys. Rev.* **167**, 331 (1968).
- ³⁸P. Morel and P. W. Anderson, *Phys. Rev.* **125**, 1263 (1962).